JOURNAL OF MATERIALS SCIENCE 15 (1980) 1207–1223

Atomically sharp cracks in brittle solids: an electron microscopy study

B. R. LAWN
Department of Applied Physics, School of Physics, University of New South Wales, Kensington, New South Wales 2033, Australia

B. J. HOCKEY, S. M. WIEDERHORN
Fracture and Deformation Division, National Measurement Laboratory, National Bureau of Standards, Washington, D.C. 20234, USA

The issue of bond rupture versus microplasticity as an essential mechanism of crack propagation in brittle solids is addressed. A detailed survey of existing theoretical and experimental evidence relating to this issue highlights the need for direct observations of events within the crack-tip "process zone", at a level approaching 10 nm. Transmission electron microscopy is accordingly used to study arrested cracks about sharp-contact (Vickers indentation and particle impact) sites in Si, Ge, SiC and Al_2O_3. The nature of the deformation which accommodates the irreversible contact impression is first investigated, in the light of Marsh's proposal of an "equivalence" between indentation and crack-tip zone processes. Interfacial and tip regions of the surrounding cracks are then examined for any trace of a plasticity-controlled fracture process. Dislocation-like images are indeed evident at the crack planes, but these are shown to be totally inconsistent with any conventional slip mechanism. The close connection between the dislocation patterns and moiré fringe systems along the cracks points to "lattice mismatch" contrast in association with a partial closure and healing operation at the interface. Analysis of all other details in the crack patterns, e.g. the presence of a crack-front contrast band indicative of a residual strain field and the disposition of interfacial fracture steps relative to the dislocation/moiré system, reinforces this interpretation. It is concluded that the concept of an atomically sharp crack provides a sound basis for the theory of fracture of brittle solids.

1. Introduction

Despite a proliferation of studies on the fracture of highly brittle solids, notably ceramic materials (see, for example, [1]), remarkably little attention has been given to the crack-tip processes actually responsible for crack extension. Fracture mechanics has been dominated by the call for simple material parameters in engineering design, most readily obtained semi-empirically from macroscopic strength or crack growth observations in conjunction with some appropriate equilibrium or kinetic extension criterion. Nevertheless, in an attempt to gain some physical insight into the fundamental nature of the fracture problem, and thence to provide a scientific base for failure prediction from first principles, a number of useful crack-tip models have been developed. The evaluation of slow crack growth phenomena is perhaps the most important potential application of such models.

Leaving aside problems associated with analytical complexity, the successes of crack-tip modelling have been muted by controversy as to the very nature of the separation process. Each model is built on some basic premise which relates to a specific crack propagation mechanism. These premises derive from two distinct schools of thought: the first concerns the notion of an ideally

0022–2461/80/051207–17$03.70/0 © *1980 Chapman and Hall Ltd.*

TABLE I Parameters of materials used in this study

Material	Covalent/ionic* bond fraction	Specimen surface plane	E (GPa)	2γ (J m^{-2})	G_c (J m^{-2})	K_c (MPa m$^{1/2}$)†	H (GPa)‡	d_c (nm)§
Si	1.00/0.00	(1 1 0)	168[a]	3.4[a]	3.0[a]	0.7	9	5
Ge	1.00/0.00	(1 1 1)	140[a]	2.3[a]	2.1[a]	0.6	8	6
SiC	0.88/0.12	(0 0 0 1)	470[b]	10[b]	20[b]	3	27	22
Al_2O_3	0.37/0.63	(1 0 $\bar{1}$ 0)	425[c]	7.0[c]	14[c]	2.2	20	20
SiO_2	0.49/0.51	amorphous	70[d]	1.8[d]	7[d]	0.7	6	14

* From Pauling's electronegativity tables [53].
† From $K_c = [G_c E/(1-\nu^2)]^{1/2}$, $\nu \approx 0.25$.
‡ Vickers indentations, this study.
§ Equations 1 to 3.

[a] [54].
[b] [55].
[c] [56].
[d] [57].

sharp crack in which fracture proceeds by the sequential rupture of cohesive bonds across a separation plane, thereby creating new surface area in a near-reversible manner; the second school takes note of the undisputed existence of a macroscopic "plastic" zone about cracks in engineering metallic and polymeric materials, and asserts that ceramic materials must behave similarly, albeit on a microscale. The issue is one of brittleness versus ductility in the crack-tip process zone [2].

The controversy between the two schools is the inevitable product of a lack of definitive evidence. With ceramics one is concerned with events over distances $\approx 10\,\text{nm}$ from the crack tip, a scale beyond the limits of resolution of conventional techniques used in observing cracks. Thus it is that the evidence presented in support of either of the two alternatives has invariably been circumstantial. A key example is the contention by proponents of the plasticity models that the existence of a residual deformation impression in a hardness test with a sharp indenter implies the operation of a similar deformation process at crack tips [3]: taken to its local conclusion, this analogy identifies hardness as a controlling material parameter in the fracture of brittle solids.

In this paper the validity of the two basic types of crack-tip models is critically examined in the light of transmission electron microscope (TEM) observations in a range of hard single-crystal materials, Si, Ge, SiC and Al_2O_3, covering a spectrum of covalent/ionic bond types.* Pertinent properties of these crystals, together with those of glass, are listed in Table I for later reference. Characteristic deformation/fracture patterns about Vickers diamond pyramid impressions conveniently permit the simultaneous study of process zones about both indentations and crack tips [4]. The study highlights the need for caution in adapting indentation data to interpret crack-tip behaviour: with due allowance for this need, the weight of the TEM evidence favours the sharp-crack picture for brittle solids.

2. Crack-tip models and indentation deformation

2.1. Continuum models of crack-tip process zones

The simplest crack-tip models are based on the continuum concept of matter. Modern-day continuum fracture mechanics ([5], Chs. 3, 4) takes an ideally Hookean crack system as its starting point, and, via the formalism of linear elasticity theory, produces convenient parameters (e.g. crack-extension force G, stress-intensity factor K) for characterizing a driving force for fracture. Taken together with some suitable criterion for crack growth, so-called linear fracture mechanics provides a theoretical framework for analysing the evolution of macroscopic fracture in a vast range of structural configurations. However, while it lends itself admirably to engineering design, the linear hypothesis runs into trouble in any description of crack extension at the microscopic level: it leads to singularities in stresses and strains at the crack tip, where the essential processes of material separation must operate. This difficulty simply reflects the fundamental non-linearity of the crack-tip problem – the separation of material inevitably involves the breaking of atomic bonds, so Hooke's law necessarily breaks down in the critical region.

The accommodation of a non-linear element into the description is achieved with minimum complication by means of the Irwin–Orowan "small-scale zone" postulate [6]. This scheme eliminates the crack-tip singularities, yet preserves the important linear fracture mechanics parameters. Non-linear separation processes are considered to be confined within a small domain (small cf. macroscopic dimensions of crack system) immediately encasing the crack tip (Fig. 1). In this description the outer, surrounding linear elastic material has the role of transmitting the system applied loading to the inner, crack-tip process zone. Theories of fracture at the mechanistic level then reduce to descriptions of the non-linear events operating within the process zone.

In this context, two basic types of nonlinear process have been proposed for equilibrium cracks:

(i) near-reversible bond rupture ("brittle" solids), in which crack extension proceeds via the sequential rupture of cohesive bonds at the crack tip. The continuum picture is one of creation of new surface area [7], i.e. $G_c \approx 2\gamma$, where G_c is the critical crack extension force and γ is the reversible surface energy. The crack-tip configuration may be regarded as "atomically sharp";

(ii) highly dissipative plastic yielding ("plastic" solids), in which extension proceeds via ductile tearing of material within the crack-tip zone. The

*Si and Ge are, of course, slightly metallic in the bonding.

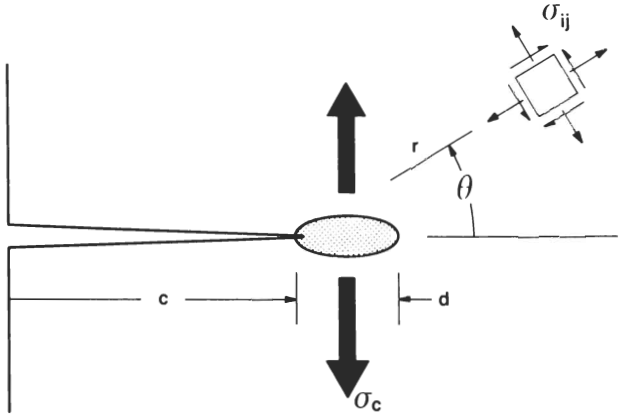

Figure 1 Parameters of crack-tip zone model.

energy expended in this mode is usually much greater than the reversible surface energy, i.e. $G_c \gg 2\gamma$. The plasticity effectively "blunts" the crack tip. Division into these two process types is more than a mere exercise in materials classification. The bond-rupture mode implies fracture controlled by *surface* properties, the plastic-separation mode by *bulk* properties. Such a distinction is vital in any extension of fracture theory to kinetic effects in crack growth.

A particularly useful refinement of the Irwin–Orowan postulate is the Dugdale–Barenblatt crack-tip model, proposed independently by Dugdale [8] for plastic process zones and Barenblatt [9] for brittle process zones. Based on the simplifying approximation of an ideally narrow zone geometry, the equilibrium requirements for a crack of length c lead to a critical zone size

$$d_c = A(K_c/\sigma_c)^2 \quad (d_c \ll c), \qquad (1)$$

where $K_c = [G_c E/(1-\nu^2)]^{1/2}$ is the critical stress-intensity factor or plane-strain toughness (E = Young's modulus, ν = Poisson's ratio), σ_c is the crack-tip tensile stress, and A is a constant $= \pi/8$ in the approximation of σ_c uniform over the zone length. In the case of brittle solids σ_c identifies with the theoretical cohesive strength, in plastic solids it identifies with the yield stress. While both these "cut-off" stresses must ultimately be determined at the atomic level, the Dugdale–Barenblatt model is strictly a product of continuum mechanics. Equation 1 does not take into account crystallographic anistropy in mechanical properties, but nevertheless serves as a useful indicator of the scale of non-linear crack-tip processes. We shall look more closely at the relation between d_c and σ_c later in Section 2.4.

On the basis of the above classification there is little doubt that most engineering metallic and polymeric materials fracture according to a plastic crack-tip separation process, G_c being typically several orders of magnitude in excess of 2γ. With ceramic materials, however, the classification is not at all clear cut: measured values of G_c approach predicted values of 2γ, typically to within a factor of two or three (Table I), but uncertainties in both experiment and theory usually preclude definitive conclusions. Thus whereas some authors (e.g. Marsh [3], in the case of glass; Petch [10], sapphire) suggest the fracture energy evidence supports the plastic-zone hypothesis, others (e.g. Hillig [11], glass; Wiederhorn *et al.* [12], sapphire) favour the bond-rupture mechanism.

2.2. Atomistic models of crack-tip process zones

The emergence of crack-tip models incorporating details of atomic structure has added considerable fuel to the brittleness argument ([5], Ch. 7). The basic approach is to set up a structure in which point masses (atoms) are held together by non-linear springs (cohesive bonds) in an appropriate array, and then to look for equilibrium configurations when the structure contains a crack and is loaded at its boundaries. If a given structure cannot sustain an atomically sharp crack without spontaneous shear instability in the near field of the tip during extension through one lattice spacing, the fracture is essentially plastic.

The first models along these lines considered the response of several crystal structures to elastic crack-tip stresses, but used conventional linear, isotropic, continuum mechanics to evaluate the stress field itself (quasi-atomistic approach). Kelly

et al. [13] proposed that fracture would be plastic if the theoretical cohesive strength of the structure in shear (favouring off-plane slip deformation) were to be exceeded before the cohesive strength in tension (favouring in-plane crack extension). Rice and Thomson [14], in a refinement of this concept, suggested that the nucleation of dislocations (or some analogous shear defect in non-crystalline solids) at the crack tip is a necessary but not sufficient condition for a ductile mode of rupture: such dislocations must also be able to propagate into the surrounding crystal, and for this to occur an energy barrier may have to be surmounted. These latter authors added the further requirement that "in order for a dislocation to blunt a crack, it is necessary for the Burgers vector to have a component normal to the crack plane, and for the slip plane to intersect the crack line (or crack front) along its whole length, i.e. the crack line must be contained within the slip plane". In the Rice and Thomson model an ideally plastic solid is then one in which the emission of blunting dislocations occurs spontaneously. With due allowance for a number of simplifying assumptions implicit in their models, Kelly *et al.* (with Rice and Thomson somewhat more emphatic) concluded that solids with strong covalent and ionic bonding may well be capable of sustaining perfectly brittle cracks, whereas solids with metallic or secondary bonding in general would not: b c c metals occupy the uncertain middle ground.

The development of fully atomistic crack-tip models has been slow for want of suitable techniques for handling a complex non-linear, many-body problem. Thomson and co-workers [15, 16] adopted the approach of constructing oversimplistic one- and two-dimensional lattices with linear force laws to a cut-off (rupture) limit, for which analytical solutions could be obtained. In sacrificing structural reality their models provided physical insight into the nature of crack stability over atomic displacements. It was found that brittle cracks tend to become "lattice trapped": i.e. there is an energy barrier to the breaking (or remaking) of individual bonds at the crack tip, such that the fracture surface energy measured experimentally will tend to be somewhat greater (depending on the nature of the bonding) than the true, reversible surface energy. Computer relaxation calculations, by incorporating more detailed (albeit empirical) non-linear force functions into the formalism, reaffirmed the basic findings of the lattice trapping models for more realistic atomic structures. In simulations of the covalent diamond-type crystals [17, 18] crack extension by discrete bond popping was found to be stable against dislocation generation. On the other hand, in simulations of b c c iron [19] the competition between bond rupture and dislocation generation was more difficult to resolve.

Thomson [2, 20], in reviewing the current understanding of crack-tip micromechanics, places great emphasis on the original Griffith concept of an atomically sharp crack as the cornerstone of fundamental fracture theory. A ratio $G_c/2\gamma$ somewhat greater than unity does not necessarily imply the existence of crack-tip plasticity, as lattice-trapping effects are capable of dissipating some energy. Moreover, dislocation activity does not in itself establish plastic rupture as the essential fracture process: provided the dislocations do not blunt the tip, the sharp-crack concept remains intact. The culmination of this reasoning is Thomson's theory of crack growth in high-strength steels [21]. Whereas the surrounding crack-tip field in these materials is undeniably governed by extensive flow processes, the strain-hardening characteristics restrict the activity of blunting reactions at the highly strained crack-tip bonds. In this way Thomson concludes that surface adsorption effects may well play a dominant role in the hydrogen embrittlement of steels. It is this same reasoning which provides the justification for more generalized theories of kinetic crack growth in terms of chemically-assisted bond rupture [22, 23].

It should be re-emphasized here that the general crack-tip problem lies beyond the scope of exact theoretical analysis. Our knowledge of the non-linear processes of material separation within the crack-tip zone, including bond rupture, is largely empirical. In setting up any model it is necessary to specify boundary conditions to accommodate the applied loading on the crack system, and the manner in which these conditions are implemented can introduce artificial constraints on the zone boundary. Most calculations pre-suppose an essentially static lattice, and so reflect strictly on low-temperature fracture behaviour. Such limitations in process-zone modelling need to be borne in mind when asserting that certain materials are capable of sustaining fully brittle cracks.

2.3. Experimental evidence on the nature of crack-tip processes

In favourable cases one can learn a great deal about the mode of fracture from an examination of markings on the separated crack surfaces ("fractography"). Thus with most metallic and polymeric materials the crack surfaces are characteristically rough, and elementary strain-sensitive techniques such as X-ray diffraction, optical microscopy, etching, etc., reveal definite evidence of a traced-out layer of gross deformation marking the passage of the crack-tip zone. With ceramic materials, however, the situation is not so well defined. In particular, single crystals and homogeneous glasses show characteristically smooth fractures, typically with cleavage steps as the major structural detail on otherwise mirror-like surfaces (at least at room temperature and low crack velocity). The cleavage steps themselves show interesting sub-structural features interpreted by some as an indication of local plastic flow, but all such features can be unequivocally demonstrated to arise from secondary fracture at the advancing crack tip [24]. Dislocation arrays have been detected on fresh cleavage surfaces and around arrested crack tips of a number of softer ceramic materials, primarily by etch methods [25]. However, a most comprehensive study by Burns and Webb [26, 27] on lithium fluoride cleavage suggests a non-blunting dislocation mechanism in which the elastic field of an advancing crack activates pre-existing sources and forms an atmosphere of dislocations which trails along behind the tip. Materials with a greater component of covalent bonding show no fractographic features at all which might be associated with crack-tip plasticity. Of course, in view of the small size predicted for the crack-tip zone in the typical ceramic (Table I), this lack of definitive fractographic evidence is not altogether surprising.

Marsh [3], in advancing his case for a ductile mode of fracture in glass, cited the following supporting evidence: (i) the high fracture energies measured in crack propagation studies (see Section 2.1); (ii) the failure of glass to attain the theoretical limit in strength; (iii) the failure of fast-running cracks to attain the predicted terminal velocities; (iv) the observation that glass can indeed be made to deform plastically under high confining pressures; (v) the existence of permanent deformation at hardness impressions and scratches; (vi) the absence of full closure and healing when an applied load is released from an incompleted fracture. However, Hillig [11] pointed out that Marsh's evidence could be given an alternative interpretation: (i) fracture parameters such as fracture energies, theoretical strengths and terminal velocities are not known with sufficient accuracy to test any crack-tip hypothesis; (ii) the fact that plastic flow does occur under high pressures does not imply that a similar process will occur at crack tips, where the stresses are tensile; (iii) frictional heating during indentation or scratching could account for a localized softening of glass, such that viscous processes might operate; (iv) hardness impressions result from complex processes that involve densification of the glass structure as well as plastic flow; (v) the wedging of debris at crack interfaces could prevent closure and healing. While specifically directed to glass, the arguments of Marsh and Hillig carry over to ceramics in general.

Thus it is seen that the available evidence for crack-tip plasticity in ceramic materials is purely circumstantial in nature. A general lack of knowledge of yield properties in this class of materials serves only to compound the existing controversy. Because of their very brittleness, ceramics, especially those with a large component of covalent bonding, tend to fail catastrophically before the onset of yield, except in complex test arrangements in which confining pressures are used to suppress crack growth. It is in this context that the indentation hardness test, where large components of hydrostatic compression and shear stress are generated locally about the test site, has emerged as a most convenient tool for characterizing the deformation properties of highly brittle solids. It is the relevance of the indentation behaviour to events within the crack-tip zone which really forms the crux of the Marsh hypothesis, and which accordingly remains to be satisfactorily discounted by those who advocate a bond rupture mode of fracture.

2.4. Correspondence between crack-tip and indentation process zones

Let us take a closer look at the correspondence between the process zones associated with crack tips (Fig. 1) and hardness impressions (Fig. 2). For this purpose it is useful to refer to the unmodified linear elastic stress fields about the singularity centres in the two situations. In the context of the Irwin–Orowan hypothesis outlined in Section 2.1 these fields then give some indication of the forces

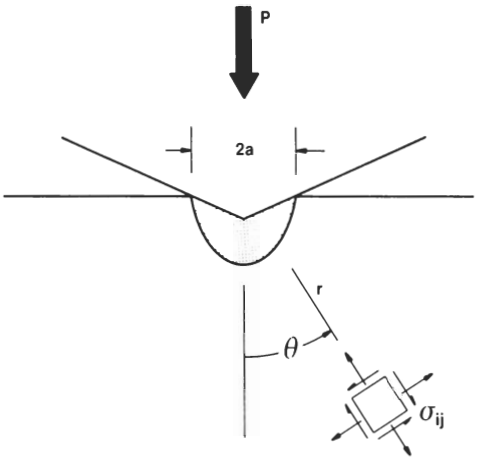

Figure 2 Parameters of indentation zone model.

transmitted to the prospective inner-zone domains. Disregarding possible complications due to mechanical anisotropy, the components of stress are of the following simple polar forms: for the crack tip, $\sigma_{ij} = Kf_{ij}(\theta)/2\pi r)^{1/2}$ (e.g. [5], Ch. 3); for the hardness impression, $\sigma_{ij} = Pg_{ij}(\theta)/\pi r^2$, where P is indenter load [28]. The angular distribution functions $f_{ij}(\theta)$ and $g_{ij}(\theta)$ are plotted in Fig. 3 for three stress components pertinent to this discussion, namely the tangential tensile stress (component associated with activation of possible fracture mechanisms), the maximum principal shear stresses (associated with plasticity) and the hydrostatic compressive stresses (associated with compaction).

The justification for any crack-tip plasticity model based on indentation behaviour essentially derives from one important similarity in the two fields of Fig. 3 – a large, common component of shear. It is this "correspondence" which effectively underlies Marsh's approach in relating crack-tip processes in glass to the "yield" processes beneath a hardness impression. Starting with the assumption that highly elastic materials deform beneath an indenter by a mode of radial flow akin to that around an expanding spherical cavity in an infinite medium, Marsh determined a semi-empirical relation between the hardness H and yield stress Y

$$H/Y = B_{E/Y,\nu} \tag{2}$$

where

$$B_{E/Y,\nu} \approx 0.28 + \{0.6/[1 - 2(1 - 2\nu)(Y/E)]\}$$
$$\times \ln \{(E/Y)/[3(1 - \nu) - 2(1 + \nu)(1 - 2\nu)(Y/E)]\}$$

is a material constant. Then identification of the cutoff stress σ_c in Equation 1 with Y in Equation 2 gives the zone site for an equilibrium crack directly in terms of H:

$$d_c = C_{E/Y,\nu}(K_c/H)^2, \tag{3}$$

with $C = AB^2$ another material constant. Marsh went on to note that hardness tends to decrease with duration of indentation, and suggested that the associated time dependence of d_c in Equation 3 could account for the static fatigue behaviour of glass. Weidmann and Holloway [29] and later Williams and Marshall [30], using data from a comprehensive kinetic study of the hardness of glass [31], developed this idea into a quantitative theory of kinetic fracture; these authors invoked the assumption that crack velocity is determined by the virtual rate of extension in critical zone length at any given value of the stress-intensity factor. Since hardness has also been found to depend on indentation time in a wide range of non-metallic solids [32], the implications of this phenomenological fatigue model extend beyond the case of glass.

The point at issue here is, just how far may one take the crack-tip/indentation analogy? For as we have already seen in outlining Hillig's objections to the crack-tip plasticity concept (Section 2.3)

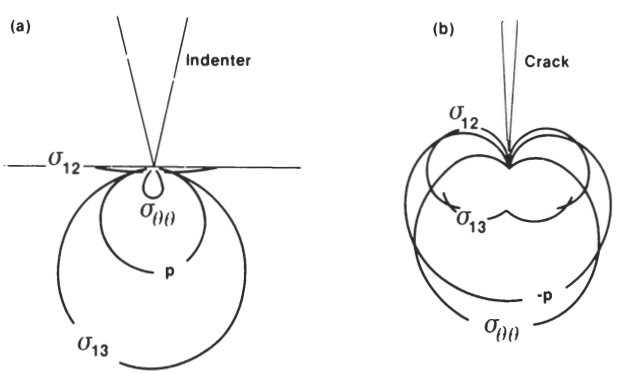

Figure 3 Linear elastic stress fields about (a) sharp indenter, (b) sharp crack, in approximation of isotropic continuum. Curves are contour plots of tangential tensile stress $\sigma_{\theta\theta}$, principle shear stress $\sigma_{13} = \frac{1}{2}(\sigma_1 - \sigma_3)$ or $\sigma_{12} = \frac{1}{2}(\sigma_1 - \sigma_2)$, and hydrostatic compressive stress $p = -\frac{1}{3}(\sigma_1 + \sigma_2 + \sigma_3)$, where principal normal stresses are defined such that σ_2 is normal to plane of diagram and $\sigma_1 > \sigma_3$ everywhere.

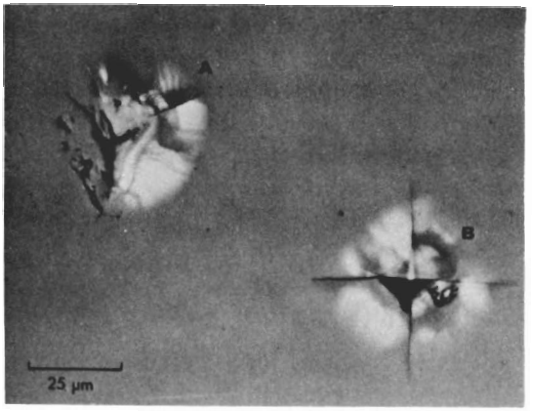

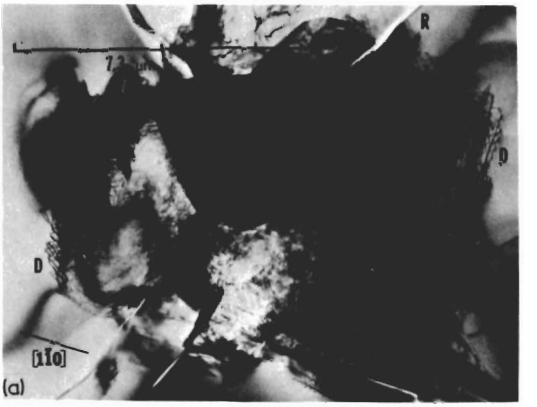

Figure 4 Comparison of surface damage pattern produced in SiC by (a) particle impingement (150 μm SiC grit at 90 m sec^{-1}) and (b) quasi-static indentation (Vickers diamond pyramid at 4.00 N). Optical micrograph, reflected light. (After [38].)

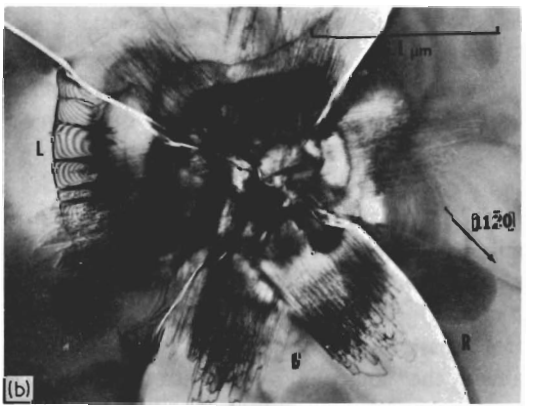

there exist some important differences as well as similarities in the two situations. First, while both stress fields in Fig. 3 indeed contain significant components of shear, the ratio shear/tension differs greatly; in terms of the Kelly–Tyson–Cottrell concept of the process zone as a competition between local fracture and flow (Section 2.2), the tendency to plasticity will be considerably less marked at crack tips than at indentations. Second, the sign of the hydrostatic stress component is opposite in Fig. 3a and b; it is possible that pressure-induced structural densification could make a significant contribution to a residual hardness impression, as is believed to be the case in high-silica glasses [33, 34], but not to crack-tip deformation. Third, the notion of a "critical" zone size d_c, so essential to the crack-tip plasticity models, does not appear to carry over to the indentation zone; in the latter case the characteristic dimension a is observed to grow without limit as indenter load P increases (Fig. 2), in accordance with the standard hardness relation

$$a = (P/\Lambda\pi H)^{1/2}, \qquad (4)$$

where Λ is a constant of indenter geometry (e.g. for a Vickers diamond pyramid indenter where a is taken as the half-diagonal of the impression, $\Lambda = 2/\pi$) (cf. d_c listed in Table I with a values marked in Fig. 5). Such considerations place an onus on any proponent of the Marsh hypothesis to produce definitive evidence for the equivalence between crack-tip and indentation processes.

Figure 5 Transmission electron micrographs of Vickers deformation/fracture patterns in (a) Si, (1 1 2) surface, at 1.00 N, (b) SiC (0 0 0 1) at 2.00 N, (c) Al_2O_3 (1 1 $\bar{2}$ 0) at 2.00 N, room temperature specimens. Note deformation elements D (dislocations) and T (twins), fracture elements L (lateral cracks) and R (radial cracks). Scale markers in this figure correspond in length to measured deformation zone parameter a (see Fig. 2). (Fig. 5b, after [4].)

3. Transmission electron microscopy

The ideal experiment for deciding the question of brittle versus ductile process zones would involve a direct observational technique capable of resolving crack-tip detail on a scale small compared with the zone dimension d_c (i.e. almost at the atomic level) during fracture evolution. None of the experimental studies alluded to in our brief survey of existing evidence (Section 2.3), with one exception, remotely approaches this stringent prescription. The exception is the work of Burns and Webb [27] on lithium fluoride, in which replicas of decorated cleavage surfaces were examined by electron microscopy. More recent work used thin-foil TEM to analyse the fracture patterns associated with residual small-scale indentations in sapphire and silicon carbide [4, 12]. The TEM studies show that we have a tool with the potential of revealing fine structure, close to the necessary level of resolution, of fresh cleavage faces, and also of the tips at arrested cracks, if not at propagating cracks. In this context it is worth noting that when dislocation sources do not operate in crack-tip fields, their activity is generally strongest at arrest positions in the fracture [25–27].

In the present study thin-foil TEM is used to examine indentation fractures in the single crystals listed in Table I. The diffraction contrast mode of imaging does of course preclude observations in glass; we can only resort to strong parallels between the documented fracture behaviour of crystalline and non-crystalline solids in drawing general conclusions from the TEM evidence on the nature of process zones. We focus our attention here on geometrical aspects of the crack patterns rather than on diffraction-contrast effects: the latter form a study in their own right, and will be discussed in greater detail elsewhere [35].

3.1. Experimental procedure

The procedure for preparing and examining contact-damaged thin-foil specimens for TEM has been described in some detail elsewhere (4, 12, 36, 37]. Single-crystal slabs (Table I) were ground and polished (mechanically and chemically) to a thickness $\approx 100\,\mu m$. Several well-spaced indentations were then made with a Vickers diamond pyramid at loads of 0.4 to 2.0 N on a majority of the test surfaces: in this load range, indenter penetration is ≈ 1 to $4\,\mu m$ for the materials studied. On the remaining test surfaces small-scale impact impressions were produced in a controlled grit-blast arrangement, using normally incident 60 and $150\,\mu m$ SiC particles at velocities up to $100\,m\,sec^{-1}$ [38]. The scale of the surface damage in the static and impact contact levels was comparable, ≈ 10 to $50\,\mu m$ (Fig. 4). Most of the specimens were prepared at room temperature, but a selected few were either annealed after indentation or impacted at high temperature. Ion bombardment was then used to thin the specimens. Most of the thinning was done from beneath the indentations, but a thin layer $\approx 1\,\mu m$ was also removed from the top surface to eliminate spurious handling damage. The resulting foils, $< 1\,\mu m$ thick, were examined in a 200 kV electron microscope.

3.2. Basic deformation/fracture morphology at contact sites

At all contact sites examined in the TEM, over 300 in total, characteristic deformation/fracture patterns were observed. Typical examples of room temperature indentations in silicon, silicon carbide and sapphire are shown in Fig. 5. Fig. 6 shows impact damage on a silicon surface at 500° C. The basic features of these patterns are readily demonstrated [4] to be consistent with macroscopically observed sharp-indenter behaviour in brittle solids. A schematic of the damage geometry relative to the specimen foil is given in Fig. 7. Thus at each contact site one may identify a central deformation zone associated with the hardness impression, surrounded by a configuration of deformation-induced tensile cracks.

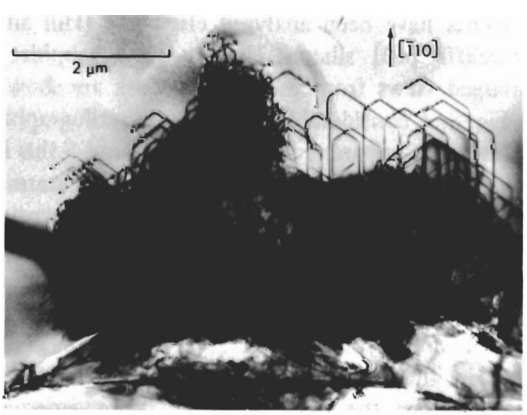

Figure 6 Transmission electron micrograph of deformation/fracture pattern in Si (1 1 0) impacted with $60\,\mu m$ SiC particle at $54\,m\,sec^{-1}$, specimen at 500° C. Note crystallographic alignment of punched-out dislocations.

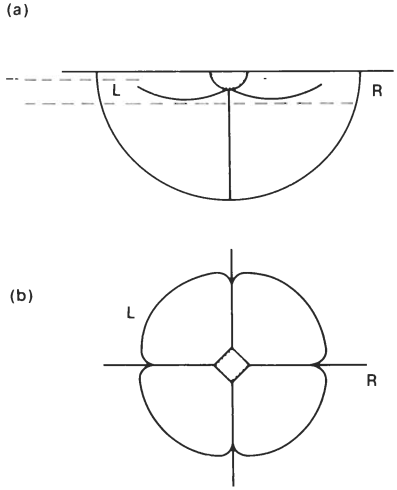

Figure 7 Schematic of Vickers deformation/fracture pattern sampled by thin foil (broken lines) for electron microscopy, showing (a) section and (b) plan views. Note central deformation zone (shaded central region) surrounded by ribbon-like radial (R) and near-planar lateral (L) cracks. (After [4].)

The central deformation zone is a facet of the indentation pattern in highly brittle solids which has been given some attention by electron microscopists [36–40]. Generally, intense diffraction contrast is always observed about the immediate contact site. In the present study some broadening of diffraction spots occurred in traversing the electron beam across this region. This is indicative of a gross structural disruption about the sharp contact point. At the periphery of the damage area it becomes possible to resolve images of the typical shear elements of crystal plasticity, dislocations, slip bands, twins, etc. These shear elements have been analysed elsewhere (Hill and Rowcliffe [40] silicon; Hockey [36], sapphire). Enlarged views from the present work are shown in Fig. 8. A considerable degree of crystallographic influence is apparent in the slip patterns – this is especially pronounced in the high-temperature impact situation of Fig. 6, where substantial relaxation of the dislocation configuration has occurred (cf. Fig. 5a). One important implication here is that individual dislocations or twins may extend well beyond the hardness impression [41]. That is, the macroscopic zone size parameter a evaluated on the basis of ideally homogeneous, isotropic deformation must be expected to underestimate the extent of slip at the microscopic level (Fig. 5).

Turning to the surrounding fracture configur-

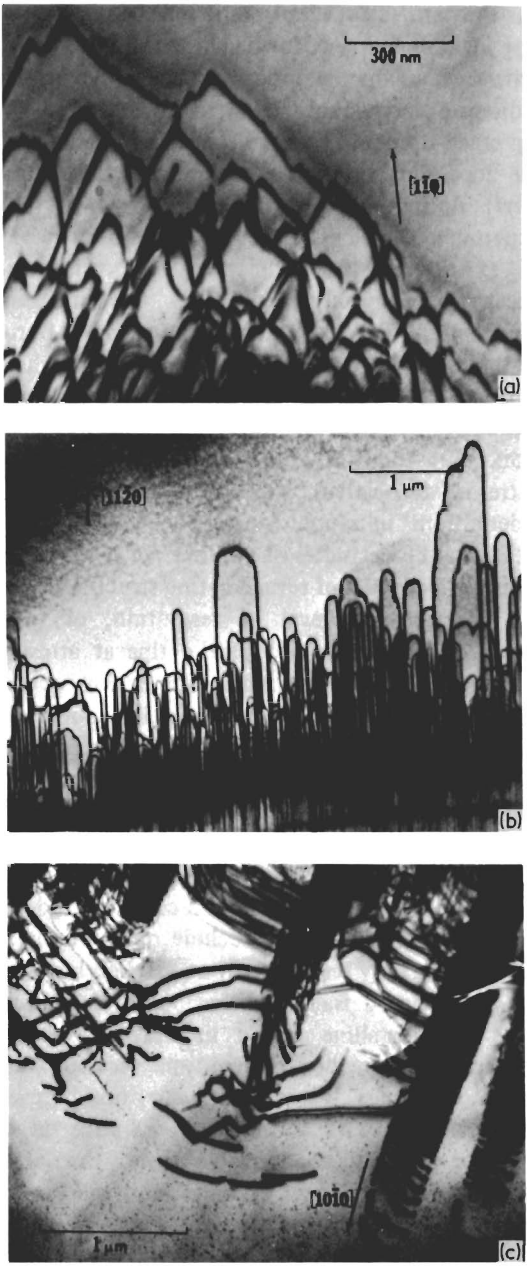

Figure 8 Details of shear elements at periphery of central deformation zone in (a) Si (1 1 2), (b) SiC (0 0 0 1), (c) Al_2O_3 (0 0 0 1), indented at room temperature.

ation, we identify two main crack types: "radial" (or "median") cracks, and "lateral" cracks (Fig. 5). Details of the evolution of these cracks systems are described elsewhere [28, 42, 43]. The radial/median system develops on symmetry planes containing the indentation axis, and accordingly manifests itself in the foil as ribbon-like segments extending radially outward from the impression.

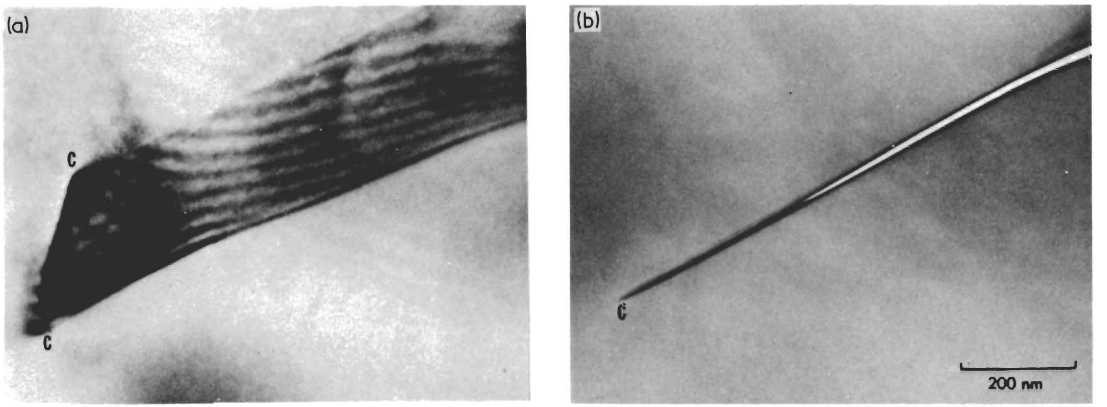

Figure 9 Radial crack segment in Si (1 1 2), particle impact specimen at room temperature, seen (a) under Läue reflection conditions and (b) tilted along crack plane. Crack-tip region designated by C.

The lateral system develops on planes roughly parallel to the indented surface, and, depending on the exact location of the foil relative to this surface, large areas of crack interface may be imaged in the electron microscope [4].

3.3. Crack–interface contrast

As pointed out in Section 2.3, dislocations or other plasticity elements generated within the process zone of an advancing crack might be expected to be left behind as subsurface deformation on either side of the newly formed interface. While the interfacial regions of arrested microcracks do indeed show a good deal of diffraction contrast in the TEM [4, 12, 44] the image details are totally inconsistent with a slip process. Here we concern ourselves with some of the more pertinent features of the interfacial images.

Most conspicuous of all the features are the fringe/network patterns which characterize lattice mismatch between diffracting crystal portions on opposite sides of the interface [4]. Typical examples are shown in Figs. 9 to 11. Diagnostic tests in the electron microscope demonstrate all contrast details in such patterns to be consistent with an interfacial closure and healing operation. Fig. 9 serves to confirm the essentially planar geometry of the patterns. Selected-area diffraction showed no evidence of structural changes, e.g. twins or phase transformations, along this or any other crack interface examined. Systematic variation of both diffraction vector and accelerating voltage lead one to diagnose the fringes as the moiré type, modulated by thickness extinction contrast at surface-inclined interfaces. In favourable cases the fringe pattern degenerates into a dislocation network, as with the micrographs from sapphire in Fig. 10: micrograph (a) illustrates

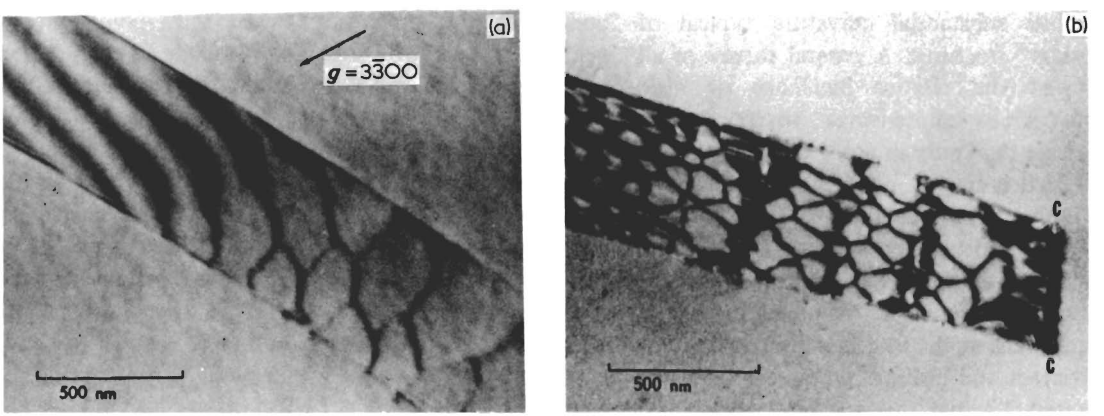

Figure 10 Radial crack segments in Al_2O_3, (a) (1 1 $\bar{2}$ 0) surface, (b) (0 0 0 1) surface, at room-temperature indentations. Crack-tip region designated by C. Note continuity between moiré fringe pattern and dislocation network, indicative of partial closure and healing at crack interface. (Fig. 10b, after [4].)

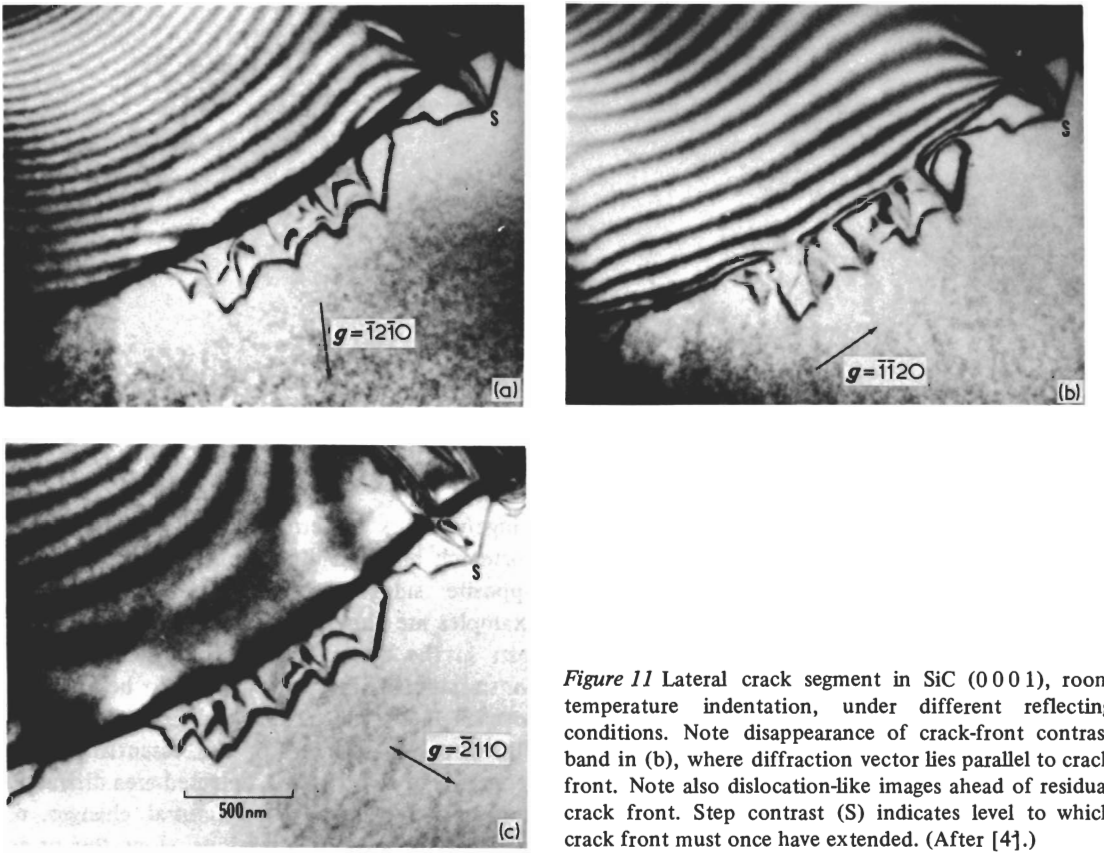

Figure 11 Lateral crack segment in SiC (0 0 0 1), room temperature indentation, under different reflecting conditions. Note disappearance of crack-front contrast band in (b), where diffraction vector lies parallel to crack front. Note also dislocation-like images ahead of residual crack front. Step contrast (S) indicates level to which crack front must once have extended. (After [4].)

this degeneration most clearly, but the relative complexity of the pattern in (b) represents the more typical observation. Systematic Burgers vector determinations indicate these dislocations, unlike those punched out around the central indentation zones, to be entirely incompatible with a primary crystallographic slip system [35]: indeed, in many instances the network interface exhibits substantial curvature typical of "conchoidal" fractures. A general survey of all cracks showed the relative incidence of dislocation-network to moiré-fringe interfacial regions to increase markedly in going from static-indentation to particle-impact contacts, and from covalence to ionicity in the bonding.

An important question which arises in connection with the issue of brittleness versus ductility is, what is responsible for preventing the opposing crack walls at the interface from making complete recontact and healing completely? We recall from Section 2.3 that this question reduces to one of resolving between the sharp-crack proposal of interfacial debris *behind* the tip and the blunt-crack proposal of irreversible deformation *at* the tip. With regard to the first of these, there is strong evidence in the micrographs that fracture steps provide the main source of closure prevention. The mechanics of step formation in terms of a crack-plane overlap process and the subsequent role of recontacting steps in producing interfacial lattice mismatch when the crack driving force is released have been discussed elsewhere [4, 45]. For the present we need only point out the incidence of fringe distortion in stepped regions in Fig. 11, and the marked absence of such regions in Fig. 10 where significant healing is observed. Another source of closure prevention is the central deformation zone itself, where elastic/plastic stresses can manifest themselves in significant residual wedging displacements at the crack mouth [46]. An investigation into the alternative hypothesis of plasticity at the crack *tip* calls for a closer look at such contrast details as are evident along the arrested fronts in Fig. 11.

3.4. Crack-tip contrast

Let us now focus attention on the actual tip regions of the indentation cracks. We may identify

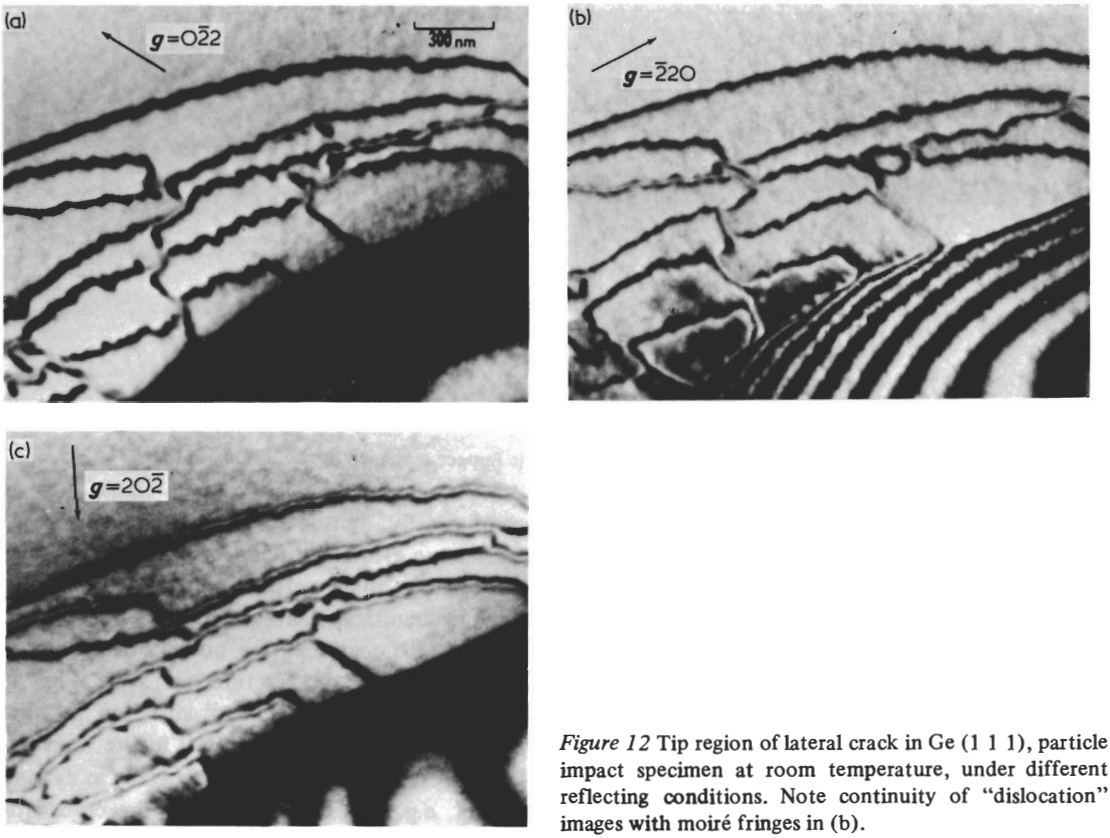

Figure 12 Tip region of lateral crack in Ge (1 1 1), particle impact specimen at room temperature, under different reflecting conditions. Note continuity of "dislocation" images with moiré fringes in (b).

two distinctive crack-front features in Fig. 11: a broad, homogeneous band of contrast up to ≈ 100 nm wide, and a configuration of dislocation-like images ahead of this band. Such features were not always evident in the micrographs (e.g. Figs. 9 and 10), depending on factors such as diffraction geometry, state of the adjoining crack interface (notably the incidence of steps), static or impact loading, etc. It was in this light that a systematic exploration of crack-tip contrast was conducted. Figs. 12 to 14 are representative examples of the observations.

The broad contrast band, which conveniently locates the existing crack front, goes out of contrast where the front lies parallel to the diffraction vector. This visibility condition, reproduced in Figs. 12 to 14, corresponds to a displacement vector normal everywhere to the front, reflecting

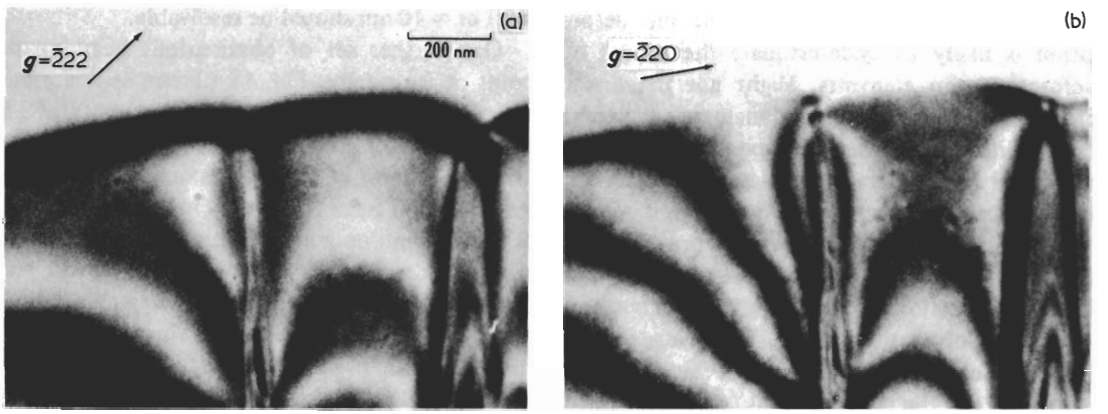

Figure 13 Tip region of lateral crack in Si (1 1 0), particle impact specimen at room temperature.

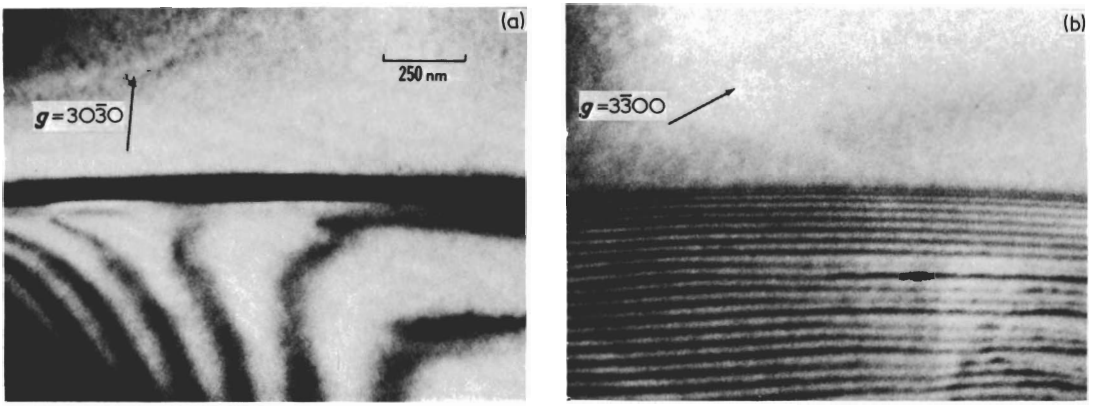

Figure 14 Tip region of lateral crack in Al_2O_3 (0 0 0 1), particle impact specimen at room temperature.

the symmetry of the plane-strain tensile fracture mode which governs the formation of indentation cracks. The contrast is indicative of a residual elastic strain field about the tip of an imperfectly closed crack. The observations accordingly follow as a logical consequence of the interfacial closure-obstruction mechanisms, and thereby lend weight to the sharp-crack hypothesis.

One might argue that the crack-front contrast band could equally well be accounted for by a core of plastic deformation located within $d_c \approx 10$ nm of the tip. In the spirit of the Dugale–Barenblatt slit-like zone model (Section 2.1), an accumulation of some 25 dislocations of Burgers vector ≈ 0.4 nm might account for such a disturbance. It is in this context that the dislocation-like images ahead of the band pointed out in Fig. 11 are of particular interest. Fig. 12 gives a more detailed view of a similar configuration in germanium. We have indicated earlier in our description of the central indentation pattern that the zone-size parameter evaluated on the basis of ideally homogeneous, isotropic deformation is likely to underestimate the extent of microscopic slip elements. Might not the linear defects in Fig. 12 represent an analogous situation in which individual dislocations extend well beyond the central core of crack-tip plasticity? After all, the presence of a strong residual stress component about an arrested crack front would provide most favourable conditions for restraining any tip-blunting dislocations from annihilating via surface-image or loop-tension forces. However, several objections can be raised against the plasticity argument: (i) the "dislocations" are contained in the plane of the crack, across which the stresses are basically tensile (although spurious shear stresses are evident in connection with crack-path disturbances, due to, for example, step-formation micromechanisms, cleavage tendencies [5], Ch. 3); (ii) the "dislocations" do not protrude beyond the extremities of fracture steps in Fig. 11, suggestive of an "overshoot" situation in which remnant healing defects are left in the wake of a slightly retracted crack front (especially in dynamic loading, e.g. Fig. 12); (iii) where the crack-front strain band is put out of contrast (Fig. 12b), the "dislocation" lines become continuous with moiré fringes behind the retracted front in the manner of Fig. 10, further supporting a closure and healing mechanism. Moreover, at crack-front regions not complicated by such overshoot phenomena, as in Figs. 13 and 14, no trace of any single element of microscopic slip is found under diffraction conditions in which the obscuring contrast associated with the residual elastic field is rendered invisible: the magnification in these micrographs is such that detail at the required level of ≈ 10 nm should be resolvable.

One further set of observations bears on the point at issue here. Fig. 15 illustrates two crack-tip regions in silicon specimens at $> 500^\circ$ C. In these instances there is clear evidence of dislocation activity at the tips, as one may have been led to expect from the analogous activity apparent at the indentation zone in Fig. 6. Of course, we are unable to make any unequivocal statement concerning the origin of the dislocations in these micrographs, e.g. whether due to intrinsic crack-tip nucleation of the type envisaged by Rice and Thomson [14] or to pre-existing sources. Nevertheless, the observations constitute a useful

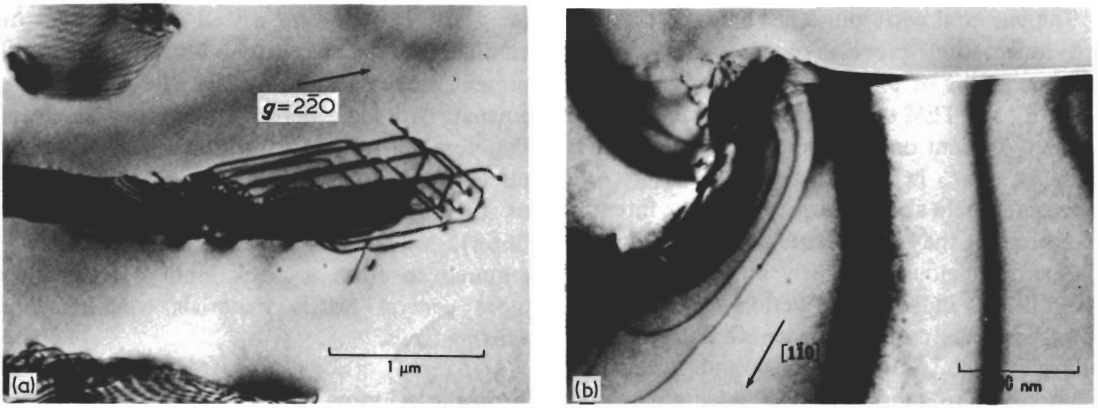

Figure 15 Crack-tip regions in Si (1 1 0), particle impact specimens (a) at 500° C, (b) at room temperature followed by anneal at > 800° C in electron microscope. Substantial dislocation activity is evident.

demonstration of the extent to which the residual field at the crack front provides an outward driving force on dislocation lines, and of the ability to resolve crack-tip plasticity elements when they do operate.

4. Discussion

In our study we have used transmission electron microscopy to provide a close view of crack-tip events in selected brittle solids. An examination of some 300 contact sites revealed no evidence to suggest that crack-tip plasticity occurs at room temperature. It has been argued that any glide dislocations emitted by an advancing crack would be subject to attractive "image" forces at the newly created fracture interface, and may therefore disappear from the crystal as the crack driving force relaxes. On the other hand, it must be noted that the intrinsic resistance to dislocation motion is high in the materials studied, particularly in the more covalent structures; in silicon and germanium, for instance, stresses approaching the theoretical shear limit are necessary to make dislocations move at all at room temperature [40, 47], and image stresses are unlikely to approach this level. Moreover, the existence of a strong residual stress field about many of the arrested crack fronts observed in this study would add significantly to the forces resisting dislocation reversibility. The observations of interfacial and crack-tip healing dislocations in Si, SiC and Al_2O_3, together with dislocation loop segments at annealed crack tips in Si, add to the conviction that the TEM study would have revealed any existing elements of crack-tip plasticity.

The crack–interface contrast patterns described in Section 3.3 bear strongly on another aspect of the crack-tip problem. According to the plasticity model an irreversible process zone would never allow the crack walls to establish full recontact (unless, of course, a reversed load was applied to the system). Whereas the observation of moiré fringe patterns is not inconsistent with this constraint, the observation of regions of interfacial healing is. The moiré-fringe/dislocation-network configuration is, on the other hand, in complete accord with the sharp-crack concept. Unless fracture steps and other structural features on opposing crack walls key together with atomic precision the interface cannot close perfectly; lattice mismatch across the interface then generates the moiré patterns. In those interfacial regions relatively free of surface detail the residual elastic stresses would drive the crack walls together near the tip until closure is at least partially complete; bond restoration then occurs, and any remaining lattice mismatch is accommodated in the form of a dislocation network as the healed interface relaxes. The process envisaged here is analogous to that of grain-boundary formation in face-to-face welding of single-crystal films [48]. It is pertinent that a greater incidence of healed crack interfaces occurred at damage sites produced in impact rather than in static contact, presumably because of the much reduced time available for contaminating gases to enter the crack and saturate the newly broken bonds [49].

The essential correspondence between crack-tip and indentation process zones implied in the Marsh concept of brittle fracture is not substantiated by the TEM study. Irreversible deformation is clearly evident on the micron scale about sharp contacts, but is undetectable down to the nanometer scale about sharp cracks. The intensity of damage in the former case is extremely high in the central regions, especially in silicon (Fig. 5a) [40, 50]. As indicated in Section 2.4, this breakdown in zone correspondence fits in with the relatively high ratios of shear and hydrostatic compression to tension in the indentation field. We are led to conclude that any observed correlation between fracture and hardness data in highly brittle solids should be regarded as no more than empirical, and therefore does not constitute a sound basis for prediction. For instance, such a correlation in the kinetics of fracture and hardness may simply reflect the fact that activated processes, perhaps totally unrelated, operate within the respective process zones.

Although the present TEM observations strictly relate to crystallite materials, there is nothing in the theoretical considerations of Section 2 to suggest that our conclusions should not be equally applicable to glassy solids. In this context it is interesting to note the following similarities in fracture behaviour between silicate glass and sapphire: (i) comparable $G_c/2\gamma$ ratios (Table I), implying similar crack-tip processes; (ii) same crack healing tendencies (cf. Wiederhorn and Townsend [49], glass; Wiederhorn *et al.* [12], sapphire); (iii) near-identical form of crack-velocity/stress-intensity-factor response in presence of water (cf. Wiederhorn and Bolz [51], glass; Wiederhorn [52], sapphire). Here, of course, we are ourselves resorting to argument of a purely circumstantial nature.

Thus the present results provide compelling, if not absolute, evidence in favour of the bond-rupture concept of fracture in highly brittle solids. This is not to imply the complete exclusion of strong interactions between fracture and plasticity processes. We have already mentioned (Sections 2.2 and 2.3) that a propagating crack may activate pre-existing dislocation sources, thereby generating a dislocation atmosphere about its tip, without suffering any blunting. Plasticity processes may play an even greater role in the *initiation* of cracks, by creating and driving incipient flaws toward a well developed fracture configuration: hence the observation in the present indentation study that the cracks always emanate from the deformation zone. There may therefore be some justification for asserting that plasticity is a necessary element in the failure of pristine materials (e.g. freshly drawn glass fibres), where some precursor mechanism is required to form a crack embryo, but not of more general brittle materials containing pre-existing flaws.

Acknowledgements

This work was sponsored by the Australian Research Grants Committee and the U.S. Office of Naval Research. The authors wish to thank Professor Sir Charles Frank, FRS, for his continued interest in this work, and for valuable comment on the manuscript.

References

1. "Fracture Mechanics of Ceramics", edited by R. C. Bradt, D. P. H. Hasselman and F. F. Lange. Vols. 1 to 4 (Plenum, New York, 1974, 1978).
2. R. THOMSON, *Ann. Rev. Mat. Sci.* 3 (1973) 31.
3. D. M. MARSH, *Proc. Roy. Soc.* A279 (1974) 420. 420.
4. B. J. HOCKEY and B. R. LAWN, *J. Mater. Sci.* 10 (1975) 1275.
5. B. R. LAWN and T. R. WILSHAW, "Fracture of Brittle Solids" (Cambridge University Press, London, 1975).
6. G. R. IRWIN, "Handbook of Physics", Vol. 6 (Springer, Berlin, 1958) p. 551.
7. A. A. GRIFFITH, *Phil. Trans.* A221 (1920) 163.
8. D. S. DUGDALE, *J. Mech. Phys. Solids* 8 (1960) 100.
9. G. I. BARENBLATT, *Adv. Appl. Mech.* 7 (1962) 55.
10. N. J. PETCH, "Fracture", edited by H. Liebowitz, Vol. 1, (Academic Press, New York, 1968) Ch. 5.
11. W. B. HILLIG, "Microplasticity", edited by C. J. McMahon (Interscience, New York, 1968) p. 383.
12. S. M. WIEDERHORN, B. J. HOCKEY and D. E. ROBERTS, *Phil. Mag.* 28 (1973) 783.
13. A. KELLY, W. R. TYSON and A. H. COTTRELL, *Phil. Mag.* 15 (1967) 576.
14. J. R. RICE and R. THOMSON, *Phil. Mag.* 29 (1974) 73.
15. R. THOMSON, C. HSIEH and V. RANA, *J. Appl. Phys.* 42 (1971) 3154.
16. C. HSIEH and R. THOMSON, *ibid.* 44 (1973) 2051.
17. J. E. SINCLAIR and B. R. LAWN, *Proc. Roy. Soc.* A329 (1972) 83.
18. J. E. SINCLAIR, *J. Phys. C: Solid State* 5 (1972) L271.
19. M. F. KANNINEN and P. C. GEHLEN, *Int. J. Fract. Mech.* 7 (1971) 471.

20. R. THOMSON, "The Mechanics of Fracture", edited by F. Erdogan, Vol. 19 (American Society of Mechanical Engineers, New York, 1977) p. 1.
21. R. THOMSON, *J. Mater. Sci.* **13** (1978) 128.
22. B. R. LAWN, *ibid.* **10** (1975) 469.
23. J. R. RICE, *J. Mech. Phys. Solids* **26** (1978) 61.
24. M. V. SWAIN, B. R. LAWN and S. J. BURNS, *J. Mater. Sci.* **9** (1974) 175.
25. J. GILMAN, *Trans. Met. Soc. AIME* **212** (1958) 310.
26. S. J. BURNS and W. W. WEBB, *ibid.* **236** (1966) 1165.
27. *Idem, J. Appl. Phys.* **41** (1970) 2078, 2086.
28. B. R. LAWN and M. V. SWAIN, *J. Mater. Sci.* **10** (1975) 113.
29. G. W. WEIDMANN and D. G. HOLLOWAY, *Phys. Chem. Glasses* **15** (1974) 68.
30. J. G. WILLIAMS and G. P. MARSHALL, *Proc. Roy. Soc.* **A342** (1975) 55.
31. S. P. GUNASEKERA and D. G. HOLLOWAY, *Phys. Chem. Glasses* **14** (1973) 45.
32. R. E. HANNEMAN and J. H. WESTBROOK, *Phil. Mag.* **18** (1968) 73.
33. F. M. ERNSBERGER, *J. Amer. Ceram. Soc.* **51** (1968) 545.
34. J. E. NEELY and J. D. MACKENZIE, *J. Mater. Soc.* **3** (1968) 603.
35. B. J. HOCKEY, unpublished work.
36. *Idem, J. Amer. Ceram. Soc.* **54** (1971) 223.
37. *Idem*, "Science of Hardness Testing and its Research Applications", edited by J. H. Westbrook and H. Conrad (American Society for Metals, Metals Park, Ohio, 1973) Ch. 30.
38. B. J. HOCKEY, S. M. WIEDERHORN and H. JOHNSON, "Fracture Mechanics of Ceramics", Vol. 3 (Plenum, New York, 1978).
39. V. G. EREMENKO and V. I. NIKITENKO, *Phys. Stat. Sol. (a)* **14** (1972) 317.
40. M. J. HILL and D. J. ROWCLIFFE, *J. Mater. Sci.* **9** (1974) 1569.
41. A. S. KEH, *J. Appl. Phys.* **31** (1960) 1538.
42. B. R. LAWN and T. R. WILSHAW, *J. Mater. Sci.* **10** (1975) 1049.
43. A. G. EVANS and T. R. WILSHAW, *Acta Met.* **24** (1976) 939.
44. L. E. MURR and W. A. SZILVA, *J. Mater. Sci.* **10** (1975) 1536.
45. J. S. WILLIAMS, B. R. LAWN and M. V. SWAIN, *Phys. Stat. Sol. (a)* **2** (1970) 7.
46. M. V. SWAIN, *J. Mater. Sci.* **11** (1976) 2345.
47. H. ALEXANDER and P. HAASEN, "Solid State Physics", Vol. 22, edited by F. Seitz and D. Turnbull (Academic Press, New York, 1968) p. 27.
48. R. W. BALUFFI, Y. KOMEN and T. SCHOBER, *Surf. Sci.* **31** (1972) 68.
49. S. M. WIEDERHORN and P. R. TOWNSEND, *J. Amer. Ceram. Soc.* **53** (1970) 486.
50. I. V. GRIDNEVA, Yu V. MILMAN and V. I. TREFILOV, *Phys. Stat. Sol. (a)* **14** (1972) 317.
51. S. M. WIEDERHORN and L. H. BOLZ, *J. Amer. Ceram. Soc.* **53** (1970) 543.
52. S. M. WIEDERHORN, *Int. J. Fract. Mech.* **4** (1968) 171.
53. L. PAULING, "The Nature of the Chemical Bond" (Cornell University Press, Ithaca, 1960) Ch. 7.
54. R. J. JACCODINE, *J. Electrochem. Soc.* **110** (1963) 524.
55. J. L. HENSHELL, D. J. ROWCLIFFE and J. W. EDINGTON, *J. Amer. Ceram. Soc.* **60** (1977) 373.
56. S. M. WIEDERHORN, *ibid.* **52** (1969) 485.
57. *Idem, ibid.* **52** (1969) 99.

Received 29 August and accepted 1 October 1979.